



The unusual kinetics of lactate dehydrogenase of *Schistosoma mansoni* and their role in the rapid metabolic switch after penetration of the mammalian host



Michiel L. Bexkens^a, Olivier M.F. Martin^b, Jos M. van den Heuvel^c, Marion G.J. Schmitz^c, Bas Teusink^b, Barbara M. Bakker^{b,d}, Jaap J. van Hellemond^a, Jurgen R. Haanstra^b, Malcolm D. Walkinshaw^e, Aloysius G.M. Tielens^{a,c,*}

^a Department of Medical Microbiology and Infectious Diseases, Erasmus MC University Medical Center, Rotterdam, The Netherlands

^b Systems Biology Lab, AIMMS, Vrije Universiteit Amsterdam, Amsterdam, The Netherlands

^c Department Biomolecular Health Sciences, Faculty of Veterinary Medicine, Utrecht University, Utrecht, The Netherlands

^d Laboratory of Pediatrics, Systems Medicine of Metabolism and Signaling, University of Groningen, University Medical Center Groningen, Groningen, The Netherlands

^e Wellcome Centre for Cell Biology, School of Biological Sciences, The University of Edinburgh, Edinburgh, United Kingdom

ARTICLE INFO

Article history:

Received 1 June 2023

Received in revised form 24 January 2024

Accepted 11 March 2024

Available online 15 March 2024

Keywords:

Schistosoma mansoni

L-Lactate dehydrogenase

Kinetics

Allosteric regulation

Glycolysis

Computer simulation

ABSTRACT

Lactate dehydrogenase (LDH) from *Schistosoma mansoni* has peculiar properties for a eukaryotic LDH. Schistosomal LDH (SmLDH) isolated from schistosomes, and the recombinantly expressed protein, are strongly inhibited by ATP, which is neutralized by fructose-1,6-bisphosphate (FBP). In the conserved FBP/anion binding site we identified two residues in SmLDH (Val187 and Tyr190) that differ from the conserved residues in LDHs of other eukaryotes, but are identical to conserved residues in FBP-sensitive prokaryotic LDHs. Three-dimensional (3D) models were generated to compare the structure of SmLDH with other LDHs. These models indicated that residues Val187, and especially Tyr190, play a crucial role in the interaction of FBP with the anion pocket of SmLDH. These 3D models of SmLDH are also consistent with a competitive model of SmLDH inhibition in which ATP (inhibitor) and FBP (activator) compete for binding in a well-defined anion pocket. The model of bound ATP predicts a distortion of the nearby key catalytic residue His195, resulting in enzyme inhibition. To investigate a possible physiological role of this allosteric regulation of LDH in schistosomes we made a kinetic model in which the allosteric regulation of the glycolytic enzymes can be varied. The model showed that inhibition of LDH by ATP prevents fermentation to lactate in the free-living stages in water and ensures complete oxidation via the Krebs cycle of the endogenous glycogen reserves. This mechanism of allosteric inhibition by ATP prevents the untimely depletion of these glycogen reserves, the only fuel of the free-living cercariae. Neutralization by FBP of this ATP inhibition of LDH prevents accumulation of glycolytic intermediates when *S. mansoni* schistosomula are confronted with the sudden large increase in glucose availability upon penetration of the final host. It appears that the LDH of *S. mansoni* is special and well suited to deal with the variations in glucose availability the parasite encounters during its life cycle.

© 2024 The Author(s). Published by Elsevier Ltd on behalf of Australian Society for Parasitology. This is an open access article under the CC BY license (<http://creativecommons.org/licenses/by/4.0/>).

1. Introduction

The lifecycle of *Schistosoma mansoni* comprises free-living and parasitic stages which encounter environmental conditions that differ in substrate availability. The free-living stages of *S. mansoni*, cercariae and miracidia, have an aerobic energy metabolism (Tie-

lens, 1994). They live in water and use as their sole energy source their endogenous glycogen stores, which are largely aerobically degraded via the Krebs cycle to CO₂, while generating ATP mainly via oxidative phosphorylation (Bruce et al., 1969; Van Oordt et al., 1989; Tielens et al., 1991). Adult *S. mansoni* worms, on the other hand, live in the bloodstream of the final host, humans. They consume glucose present in the bloodstream of this host and have, despite this aerobic environment, a fermentative metabolism, producing mainly lactate (Bueding, 1950; Tielens et al., 1989). This switch in the energy metabolism of *S. mansoni*, from an aerobic metabolism to lactate fermentation, occurs immediately after pen-

* Corresponding author at: Department of Medical Microbiology and Infectious Diseases, Erasmus MC University Medical Center, P.O. Box 2040, 3000 CA Rotterdam, The Netherlands.

E-mail address: a.tielens@erasmusmc.nl (A.G.M. Tielens).

etration of the final host. When cercariae penetrate the final host, they lose their tail and the cercarial body transforms into a schistosomulum. During this biological transformation with its many morphological and physiological changes, a biochemical transition also occurs. Schistosomula switch very rapidly to a more anaerobic metabolism, producing mainly lactate. However, the biological transformation from cercaria to schistosomulum and the biochemical switch towards fermentation are separate processes that are not necessarily linked. The increased formation of lactate is induced by the mere presence of external glucose, which results in an increased glycolytic flux (Horemans et al., 1991, 1992). The instantaneous transition to a more anaerobic energy metabolism after penetration of the host is thus not related to an inadequate availability of oxygen nor by a change in enzyme expression patterns, but is caused by the sudden increase in the availability of glucose.

Lactate dehydrogenase (LDH) catalyzes the interconversion of pyruvate and lactate. LDH is one of the best-characterized enzymes in terms of protein evolution, folding, catalytic mechanism, stability and three-dimensional (3D) structure, and this enzyme has been purified and characterized in bacteria, archaea, and eukaryotes (Birkoft et al., 1982; Madern, 2002). Here we focus on a eukaryotic fructose 1,6-bisphosphate (FBP)-sensitive LDH, discovered in the human parasitic helminth *S. mansoni* (Tielens, 1997). Its structural characteristics are compared with prokaryotic FBP-sensitive LDHs and the canonical eukaryotic orthologues that are not FBP-sensitive.

NADH-dependent L-lactate dehydrogenases (L-LDH, EC 1.1.1.27) catalyze the reversible reduction of pyruvate to lactate with the simultaneous oxidation of NADH to NAD⁺. The NADH-dependent L-LDHs form, together with NAD(P)H-dependent L-malate dehydrogenases (L-MDH), a large superfamily of dehydrogenases that have been very well characterized. NADH-dependent L-LDHs are tetrameric enzymes, where each subunit functions independently, and cooperativity between the catalytic sites is not observed. The active site of each subunit consists of a well-defined pocket (Fig. 1A). The side chains of Arg171, Gln102 and Thr250 form direct hydrogen bonds with the pyruvate substrate. Throughout this paper, numbering of the amino acids in LDH is according to Eventoff et al. (1977). Other key catalytic residues including His195, Asp 168 and Asp53 line the pocket and facilitate the transfer of electrons from the coenzyme NADH to pyruvate. Despite a relatively low amino acid sequence identity, considerable structural identity is observed between the crystal structures of LDH and MDH (Goward and Nicholls, 1994).

Many prokaryotic NADH-dependent L-LDHs are allosterically activated by fructose-1,6-bisphosphate (FBP), an intermediate of glycolysis (Garvie, 1980; Iwata and Ohta, 1993; Fushinobu et al., 1996). A few observations of FBP sensitivity of LDH in eukaryotes were reported, but these have never been pursued (Lloyd, 1983; Brennan et al., 1995; Tielens, 1997). The allosteric regulation of L-LDHs of prokaryotes, on the other hand, has been studied extensively (Iwata and Ohta, 1993; Iwata et al., 1994; Fushinobu et al., 1996) and these LDHs all consist of four identical monomers arranged around what are conventionally known as the P, Q and R axes (Adams et al., 1973). Each monomer has one active site and the tetramer has two allosteric FBP-binding sites, each situated at the interface between two monomers, which correspond to the so-called anion-binding sites of the vertebrate enzymes (Grau et al., 1981; Wigley et al., 1992). In the FBP-binding site of prokaryotic LDHs, an FBP molecule interacts with four positively charged residues, Arg173 and His188 of two juxtaposed subunits (Fig. 1B), thereby stabilizing the tetramer by forming a bridge between the subunits (Wigley et al., 1992; Iwata et al., 1994). Eukaryotic LDHs, on the other hand, have an N-terminal extension of approximately 13–20 residues, which is absent in prokaryotic

LDHs (Adams et al., 1973; Iwata et al., 1994). This N-terminal extension forms an extended conformation, wraps around the adjacent subunit in the tetramer and provides an alternative mechanism for stabilizing the tetrameric quaternary structure of eukaryotic L-LDHs (Read et al., 2001).

It has been suggested that in prokaryotes a system evolved that enables LDH to be fully active only when FBP levels are high, which is in times of high glucose availability (Wigley et al., 1992). Under less favourable nutrient conditions, LDH activity is reduced and pyruvate, instead of being converted to lactate and then excreted, enters mainly into the Krebs cycle, which results in more ATP per glucose degraded. In this paper, we propose that such a metabolic switch orchestrated by allosterically regulated LDH is not exclusive to prokaryotes but exists also in *S. mansoni*. The sensitivity of SmLDH to ATP and FBP prevents not only the inefficient fermentation of the endogenous glycogen reserves of the free-living stages but also prevents a fatal accumulation of glycolytic intermediates which would otherwise occur upon penetration of the final host, and is caused by the presence of high glucose levels in this new environment.

2. Material and methods

2.1. Parasites

The Puerto Rican strain of *S. mansoni* was maintained in Golden hamsters (*Mesocricetus auratus*) for which animal ethics approval had been obtained (license EUR1860-11709). Animal care and maintenance were in accordance with institutional and governmental guidelines. Adult *S. mansoni* worms were isolated 6–7 weeks after infection with 600 cercariae per hamster. The hamsters were anesthetized with isoflurane and perfused with 0.9% NaCl to collect the worms.

2.2. Chemicals

All chemicals used were from Sigma Aldrich, St. Louis, Missouri, United States of America unless otherwise indicated.

2.3. Purification of native lactate dehydrogenase from adult *S. mansoni* worms

After isolation from infected hamsters, the adult worms were washed in ice-cold buffer A which consisted of 25 mM imidazole (pH 7.4), 1 mM EDTA, 50 mM glucose and 20 mM thioglycerol. Worms were homogenized with an ultra-turrax in 5 ml of buffer A supplemented with 0.25 mM NADH and 2 mM FBP. The homogenate was sonicated on ice 10 times intermittently for 15 s, with a 10 s rest in between pulses, and subsequently centrifuged for 30 min at 48,000g, 4 °C. The supernatant was filtered over a fine mesh and taken up in a final volume of 20 ml of buffer A supplemented with 0.25 mM NADH and 2 mM FBP. This sample was applied to a DEAE column, which was eluted with buffer A. The fractions containing LDH activity were pooled and NADH, FBP and NaCl were added to reach final concentrations of 0.25 mM, 2 mM and 0.5 M, respectively.

A DEAE-sepharose 4B affinity column was prepared via the following procedure: AH-sepharose 4B was soaked in 0.5 M NaCl, washed over a filter with 300 ml of 0.5 M NaCl followed by 100 ml of H₂O. Potassium oxalate (1.1 g) was dissolved in 5 ml of water and added to the sepharose. N-(3-Dimethylaminopropyl)-N'-ethylcarbodiimide hydrochloride (EDC-HCl) was dissolved (0.9 g in 1.5 ml of H₂O), and added while keeping the pH at 7.5 for 75 min. The reaction was continued for 48 h while shaking gently. The sepharose was washed with acetate-buffer (0.1 M acetate,

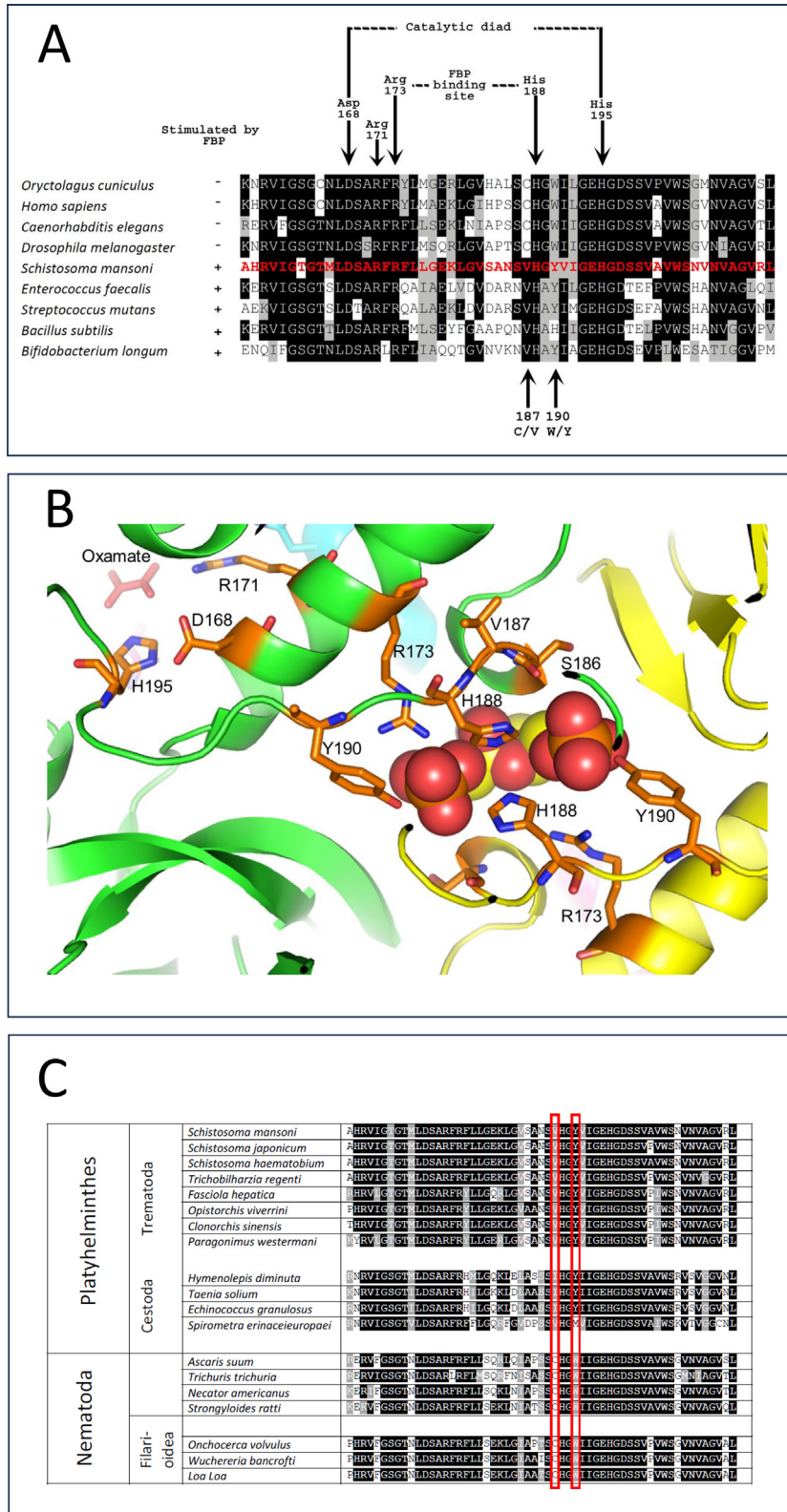


Fig. 1. Structural aspects of the active site and the fructose-1,6-bisphosphate (FBP)-binding sites of various lactate dehydrogenases (LDHs). (A) The alignment of several different LDHs. Throughout this paper, numbering of the amino acids in LDH is according to Eventoff et al. (1977). Marked with black arrows (top) are highly conserved amino acids around the active site. Above the sequence of *Schistosoma mansoni* (in red (bold grey)) four sequences are shown of LDHs of eukaryotes, while the four sequences underneath are from prokaryotic, FBP-sensitive LDHs. Black arrows (bottom) indicate amino acids 187 and 190 where the schistosomal amino acids are identical to the prokaryotic FBP-sensitive ones. Black shading indicates identity and gray shading indicates similarity. (B) A view of the FBP binding pocket and lactate (oxamate) binding site in the *S. mansoni* LDH structure (modeled on the human LDH(1t2f) crystal structure). The view is parallel to the two-fold axis relating two chains (green (medium grey) and yellow (light grey)) of the LDH tetramer. FBP is shown as spheres, and sidechains within 5 Å of the modeled FBP are drawn as sticks as are the key catalytic residues R171, D168 and H195. Both the oxamate ion which mimics the lactate substrate and FBP are from the R-state LDH structure from *Bifidobacterium longum* (1LTH) and positioned by a least-squares fit of all C α atoms. (C) An alignment of the active sites of LDHs from various Platyhelminthes and Nematoda (the same part of the enzyme is shown as in A). Red (grey) boxes indicate amino acids 187 and 190 where the ones in LDHs of trematodes are identical to those in prokaryotic FBP-sensitive LDHs, and the ones in LDHs of nematodes are identical to those in eukaryotic FBP-insensitive LDHs. Black shading indicates identity and gray shading indicates similarity.

0.5 M NaCl, pH 4) before being washed with Tris/HCl buffer (0.1 M Tris/HCl, 0.5 M NaCl, pH 8) and was washed with acetate-buffer once more. The column was rinsed with buffer A supplemented with 0.5 M NaCl, 0.25 mM NADH and 2 mM FBP before loading the *S. mansoni* sample. The column was then rinsed with 30 ml of the same buffer before starting the elution. The elution buffer was the same but now without NADH. Fractions of 1 ml were collected and screened for LDH activity.

2.4. Recombinant expression of SmLDH (r-SmLDH)

For recombinant expression of the *S. mansoni* protein lactate dehydrogenase (r-SmLDH), cDNA was prepared from RNA isolated from adult *S. mansoni* worms (Puerto Rico strain) as described earlier (van Grinsven et al., 2009). In short, worms were snap-frozen and ground up in liquid nitrogen, and dissolved in TRIzol reagent (Invitrogen, Breda, The Netherlands). Total RNA was extracted following the manufacturer's instructions and cDNA was prepared using oligo-dT primers and ImProm-IITM Reverse Transcriptase (Promega, Leiden, The Netherlands). This cDNA was used as target in a PCR with the primers SmLDHFwd (5'- **aagctagc**-atgcatctatcgatg-3') and SmLDHRev (5'- **ggatcctta**tgatggtgatggtgcccattgaccccggtat-3'). These primers contained two restriction sites, *Bam*HI and *Nhe*I (indicated in bold in the forward and reverse primer, respectively) and a 6xHIS motif, (underlined in the reverse primer). A fragment of 1063 bp was amplified and inserted in the PGEM T-EZ plasmid (Promega) after which the ligated plasmid was transformed in Top10 *Escherichia coli* cells (Invitrogen). Plasmids were screened with direct colony PCR and restriction analysis using EcoRI Fastdigest (Thermo Fisher Scientific, Breda, The Netherlands). Plasmid DNA was isolated from positive clones and the SmLDH insert was cloned in the PET11c plasmid (vector) by *Bam*HI + *Nhe*I digestion and subsequent ligation with T4 ligase (Promega). Ligated plasmids were transformed in BL21(DE3)pLysS *E. coli* for protein expression after which they were sequenced and verified by aligning them to the SmLDH sequence with accession number Smp_038950, retrieved from the Sanger SchistoDB (<https://parasite.wormbase.org/index.html>). Additionally, the sequence was translated and verified to match Uniprot primary accession number G4VQZ5.

2.5. Purification of recombinant LDH

r-SmLDH was purified from *E. coli* using a Ni-NTA Fast Kit with nickel-charged agarose beads following the manufacturer's instructions, using the provided lysis and elution buffers (Qiagen, Hilden, Germany).

After induction of expression by 1 mM IPTG (Thermo Fisher Scientific, Breda, The Netherlands) for 24 h, bacteria were pelleted by centrifugation at 4,000g for 30 min at 4 °C, supernatants were removed and the pellets were stored at –20 °C until further use. To purify the recombinant protein, the pellets were thawed and lysed in 1 ml of lysis buffer. The lysates were spun down at 15,000g for 10 min at 4 °C. Supernatants were transferred to a clean tube and 250 µl of Ni-NTA beads (Qiagen) were added. After 1 h of shaking gently at 4 °C, the beads were washed 10 times using the provided washing buffer. Elution buffer (1 ml) was applied to the beads. The supernatant was removed after 15 min of incubation, after which β-mercapto-ethanol was added to a final concentration of 0.5 mM to inhibit oxidation of SmLDH. Samples were taken before the addition of β-mercapto-ethanol to determine the protein concentration by a Lowry method as described by Bensadoun and Weinstein (1976) using BSA as a standard.

2.6. Alignments

Amino acid sequences of multiple well-characterized LDH enzymes (G4VQZ5, A0A6A5E099, A0A4Z2D9L4, A0A183VSN1, A0A075A688, Q1M156, A0A5J4NZD4, A0A2H1CIC5, E3SW74, G8ZAG6, W6UVI3, A0A0R3SK83, A0A077ZV3, A0A1I7VWP7, W2SR36, J9F0C1, C7DRP0, A0A090KRN0, F1L7Z3, P0CW93, Q27888, Q95028, Q839C1, P13491, P13714, P26283, P07195) were retrieved from Uniprot in FASTA format. Alignments were produced with ClustalW2 and scored for similarity using Boxshade server version 3.21.

2.7. Enzyme kinetics of SmLDH

The enzyme kinetics of native and recombinant SmLDH were determined by an enzyme assay monitoring, at 22° C, the oxidation of NADH to NAD⁺ at 340 nm. The assay buffer consisted of 100 mM Tris-HCl pH 7.4, 0.125 mM NADH (Roche, Basel, Switzerland), 1 mM MgCl₂, 0–2 mM Fructose-1,6-bisphosphate (FBP) and/or 0–5 mM ATP. Stock solutions of FBP and ATP were prepared in 100 mM Tris-HCl pH 7.4. In all experiments, a steady baseline was reached before starting the reaction with the addition of sodium pyruvate (16 mM final concentration or otherwise as indicated). As a control, LDH from rabbit muscle (Roche) was tested under identical conditions. All measurements were performed in triplicate, except for those performed with LDH purified from adult worms, due to the very limited availability of that sample.

2.8. 3D modelling of SmLDH

The sequence for SmLDH (NCBI Reference XP_018655219.1, Uniprot G4VQZ5) was used to carry out BLAST searches against the PDB database (Version Nov 2021). The top hit was the X-ray structure of human L-lactate dehydrogenase B complexed with NAD⁺ and 4-Hydroxy-1,2,5-Oxadiazole-3-Carboxylic Acid (PDB code 1T2F) which has 56% sequence identity and 99% coverage (332 amino acids). A tetrameric model of SmLDH was produced using the MODELLER program (Eswar et al., 2008) using the human LDH (hLDH) structure (1T2F) as a template. The root mean square displacement (RMSD) between the modeled SmLDH tetramer and the template human LDH tetramer using all four chains was 0.1 Å. A second tetrameric model was built using the X-ray structure of *Bacillus subtilis* LDH complexed FBP and NAD⁺ (PDB code 3PQD). This is the best currently available structural template for an LDH structure that is complexed with FBP and has 39.9% identity to SmLDH over its length of 326 amino acids. The RMS fit between the two tetramer models using all 1249 Cα atoms (excluding the N-terminal 30 residues) was calculated using the program SUPERPOSE (Winn et al., 2011) and gave a mean displacement of 1.7 Å. Docking studies of ATP and FBP binding to the anion pocket in the model SmLDH structure were carried out using Autodock Vina (Trott and Olson, 2010).

2.9. Kinetic modeling of the carbohydrate metabolism in *S. mansoni*

2.9.1. Model language and simulation software

Models were built in the PySCeS Model Description Language (Olivier et al., 2005) and are available via the Biomedels database with ID: MODEL2208290002 via <https://www.ebi.ac.uk/biomodels/MODEL2208290002>. All model files and scripts to obtain the model results are published on Zenodo: <https://doi.org/10.5281/zenodo.10401097>. Simulations were done in the open-source software PySCeS (version 0.9.3) (Olivier et al., 2005). Our analysis made use of the iPython console (Pérez and Granger, 2007) Jupyter

Notebooks (Kluyver, T., Ragan-Kelley, B., Pérez, F., Granger, B.E., Bussonnier, M., Frederic, J., Kelley, K., Hamrick, J.B., Grout, J., Corlay, S., 2016. Jupyter Notebooks—a publishing format for reproducible computational workflows. <https://jupyter.org/>), and the Python modules numpy (Van Der Walt et al., 2011), scipy (Jones, E., Oliphant, T., Peterson, P., 2001. SciPy: Open source scientific tools for Python. <https://scipy.org/>) and pandas (McKinney, 2011). All plots were made in R (Team, R.D.C., 2009. A language and environment for statistical computing. [https://www.R-project.org.](https://www.R-project.org/)) with help from the ggplot2 (Wickham, 2016) and data.table (Dowle, M., Srinivasan, A., 2017. data.table: Extension of ‘data. frame’. R package version 1.10. 4–3).

2.9.2. Model construction

The model building is described in detail in Supplementary Data S1, section 2. Supplementary Data S1 also includes a full description of the final model (section 3). In short, an existing yeast glycolysis model (van Eunen et al., 2012) was modified to the stoichiometry of *S. mansoni* carbohydrate metabolism (Fig. 2). Where possible, *S. mansoni* values for enzyme parameters were used. Parameters for allosteric regulation of LDH were fitted to experimental data from the current paper (Supplementary Fig. S1).

2.9.3. Steady state and time-course simulations

For each simulation, 1000 models with parameters sampled from probability distributions were generated (for details see supplementary data, Supplementary Data S1, section 2, ‘parameter sampling’), and either a steady-state solution or a time course was computed. Steady states flagged as invalid by PySCEs were discarded and in this case, a time course of 7 days duration (model time) was run and the last value was recorded as the steady-state solution. This value was chosen because no more variations could be observed by plotting concentrations over time for a model parameterized by the mean value of the posterior distribution of unmeasured parameters.

3. Results

3.1. Enzyme activity of LDH purified from adult worms

Stimulation of LDH by FBP is common in prokaryotes, but is not well characterized in eukaryotes. We investigated the kinetics of SmLDH purified from adult worms to study the effects of FBP on this enzyme. As several FBP-sensitive bacterial LDHs are inhibited by ATP, we also tested the influence of ATP on the activity of

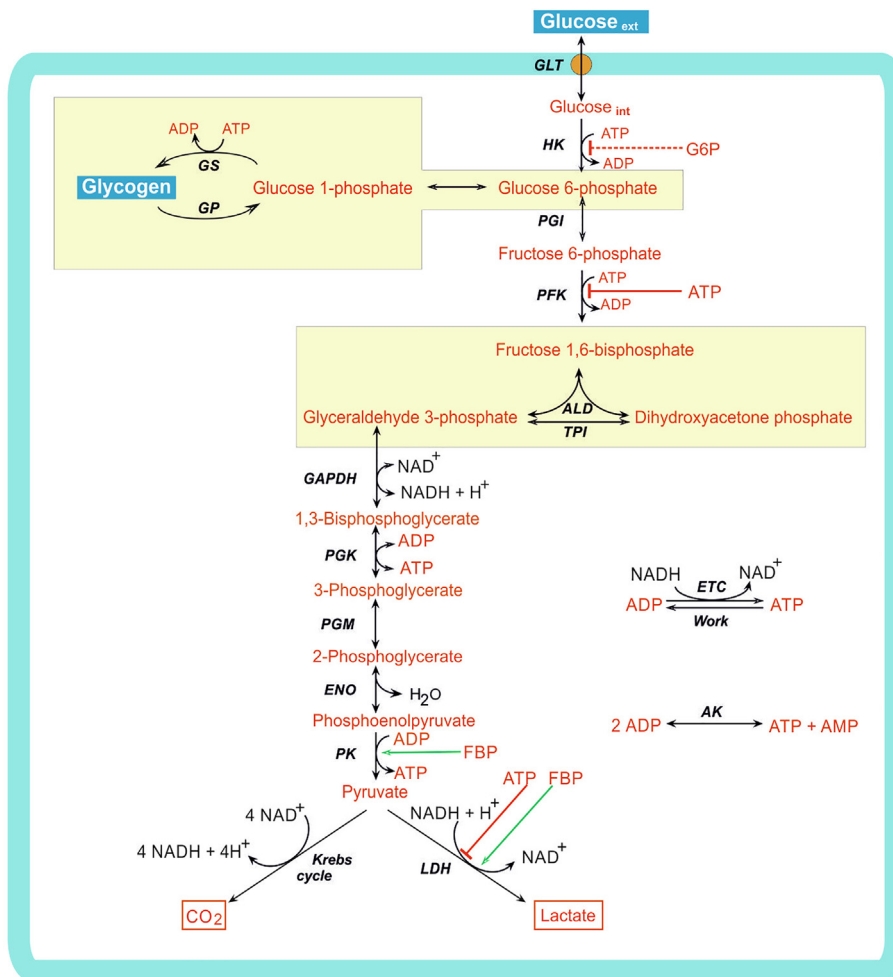


Fig. 2. Metabolic scheme of glucose and glycogen degradation by *Schistosoma mansoni*. The two yellow (grey) boxes in this scheme indicate that the reactions inside each box are modeled in the kinetic model as a single reaction. AK, adenylate kinase; ALD, aldolase; ENO, enolase; ETC, electron-transport chain; GAPDH, glyceraldehyde 3-phosphate dehydrogenase; G6P, glucose-6-phosphate; GP, glycogen phosphorylase; GS, glycogen synthase; HK, hexokinase; Krebs cycle: a simplified representation of the Krebs cycle; LDH, lactate dehydrogenase; PFK, phosphofructo kinase; PGI, phosphoglucose isomerase; PGK, phosphoglycerate kinase; PGM, phosphoglycerate mutase; PK, pyruvate kinase; TPI, triosephosphate isomerase; Work, ATP expenditure by the cell. Inhibition and stimulation of glycolytic enzyme activities are indicated with red and green (dark and medium grey) arrows, respectively. The inhibitory effect of G6P on schistosomal hexokinase is much less than the canonical inhibition of eukaryotic hexokinases and is indicated by a dashed arrow.

SmLDH (Fig. 3A). Purified SmLDH was sensitive to inhibition by ATP: 2.5 mM ATP inhibited the enzyme activity by 50%. At physiological concentrations of 5 mM ATP, only 14% of the enzyme activity remained. The addition of 2 mM FBP neutralized the inhibition incurred by ATP, and at 2.5 mM ATP it restored enzymatic activity almost to the level without ATP (Fig. 3A). In the absence of ATP, FBP also acted as an activator of SmLDH. At a concentration of 2 mM, FBP increased the specific activity of SmLDH to approximately 175% of the level without FBP (Fig. 3A). LDH from rabbit muscle was tested as a control under identical conditions and was sensitive to neither ATP nor FBP (Fig. 3B).

3.2. Alignment of LDHs

In view of the kinetic properties of SmLDH which resemble those of the FBP-sensitive LDHs of prokaryotes, we hypothesized that this peculiar FBP-sensitive eukaryotic LDH might structurally resemble prokaryotic LDH. Therefore, we looked more closely at the amino acid sequence of SmLDH and compared it with known FBP-sensitive and non-sensitive LDHs. SmLDH (G4VQZ5 Uniprot) was aligned against several prokaryotic and eukaryotic LDHs (Supplementary Fig. S2).

At first glance, SmLDH seemed to resemble standard eukaryotic LDHs. SmLDH features a 15-amino acids N-terminal extension, common in eukaryotic LDHs, which acts as an extended structure of each of the four monomers and interacts with the neighbouring subunit, stabilizing the (enzymatically active) relaxed state conformation of non-allosteric LDHs (Iwata et al., 1994). Furthermore, the universally conserved polar residues Asp168, Arg171 and His195, which play an important role in substrate binding and catalytic action, are present in SmLDH (Fig. 1A and B).

The two allosteric FBP-binding sites of FBP-sensitive prokaryotic LDHs, each situated at the interface between two monomers, correspond to the so-called anion-binding sites of the vertebrate enzymes. The binding of the respective ligands in the anion-binding site or the FBP site enhances the enzymatic activity and stabilizes the quaternary structure of the enzyme. In FBP-sensitive prokaryotic LDHs, each of the two FBP-binding sites is composed of residues from two subunits related by the P-axis, where the anion-binding site of vertebrate LDHs is located (Fushinobu et al., 1996). Arg-173 and His-188 of this site form salt bridges with phosphate moieties of the bound FBP molecule (Fig. 1A and B). Remarkably, the SmLDH residues of this conserved FBP/anion binding site show some interesting similarities and differences compared with common eukaryotic LDHs; while all

eukaryotic LDHs have Cys187 and Trp190 residues, SmLDH has Val187 and Tyr190. Intriguingly, the latter two are the same residues that are present in FBP-sensitive prokaryotic LDHs (Fig. 1A).

We then investigated the genomes of other parasitic worms (Fig. 1C) and noticed that all trematodes we sampled contained Val 187 and Tyr 190, whereas the nematodes contained Cys 187 and Trp 190.

3.3. Enzyme activity of r-SmLDH

We expressed SmLDH as a recombinant protein to allow a more thorough characterization of the kinetic properties of SmLDH. The kinetic parameters V_{max} and K_m were determined and the influence of ATP and FBP was investigated. The r-SmLDH was catalytically active and had similar enzymatic properties as the purified native SmLDH. The addition of FBP increased the affinity of the recombinant enzyme for pyruvate, the $K_m(\text{pyruvate})$ decreased from 2.7 mM at 0 mM FBP to 1.1 mM in the presence of 0.5 mM FBP (Fig. 4). The V_{max} seems to decrease slightly ($\approx 20\%$) from 79 to 63 $\mu\text{mol}\cdot\text{min}^{-1}\cdot\text{mg}^{-1}$ at increasing FBP concentrations (Fig. 4). Similar to the native SmLDH, addition of ATP had a strong inhibitory effect on r-SmLDH and decreased the V_{max} from 34 $\mu\text{mol}\cdot\text{min}^{-1}\cdot\text{mg}^{-1}$ (0 mM ATP) to 14 $\mu\text{mol}\cdot\text{min}^{-1}\cdot\text{mg}^{-1}$ (0.5 mM ATP), while the $K_m(\text{Pyruvate})$ remained constant at approximately 2.5 mM (Fig. 5). This is indicative of non-competitive inhibition by ATP.

3.4. 3D structural alignment of LDH

To investigate whether the observed differences in kinetic properties between SmLDH and canonical eukaryotic LDHs can be explained by the structural differences between these enzymes caused by the known differences in primary structures, we produced two tetrameric models of SmLDH with the MODELLER program using two different crystal structures as templates: human B-LDH (hLDH) and *Bacillus subtilis* LDH (BsLDH), which is FBP-sensitive. The two resulting tetrameric model structures of SmLDH are very similar, both in the active site and in the allosteric FBP-binding site (Supplementary Fig. S3). Comparison of the active site of SmLDH with those of hLDH and BsLDH showed no significant differences, which is not very surprising as the catalytic and substrate binding residues are highly conserved in all LDHs, prokaryotic as well as eukaryotic (Fig. 1A).

An overlay of the SmLDH model with the human LDH structure (1T2F) highlights the side chain differences in the allosteric pocket

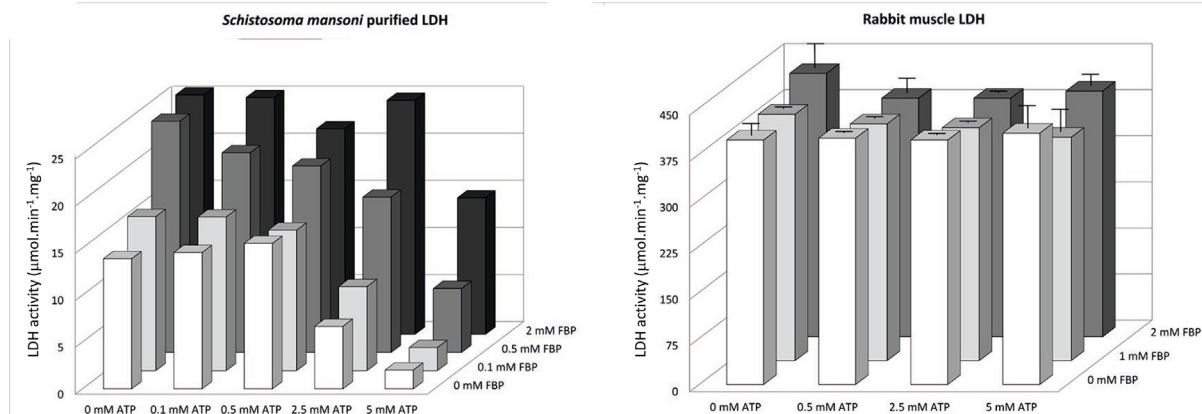


Fig. 3. The effects of fructose-1,6-bisphosphate (FBP) (0–2 mM) and ATP (0–5 mM) on the activity of lactate dehydrogenase (L-LDH) of *Schistosoma mansoni* and rabbit muscle. (A) The activity of LDH affinity-purified from adult *S. mansoni* worms (single experiment). (B) The activity of commercially available LDH from rabbit muscle; each column represents the average of three measurements \pm S.D.

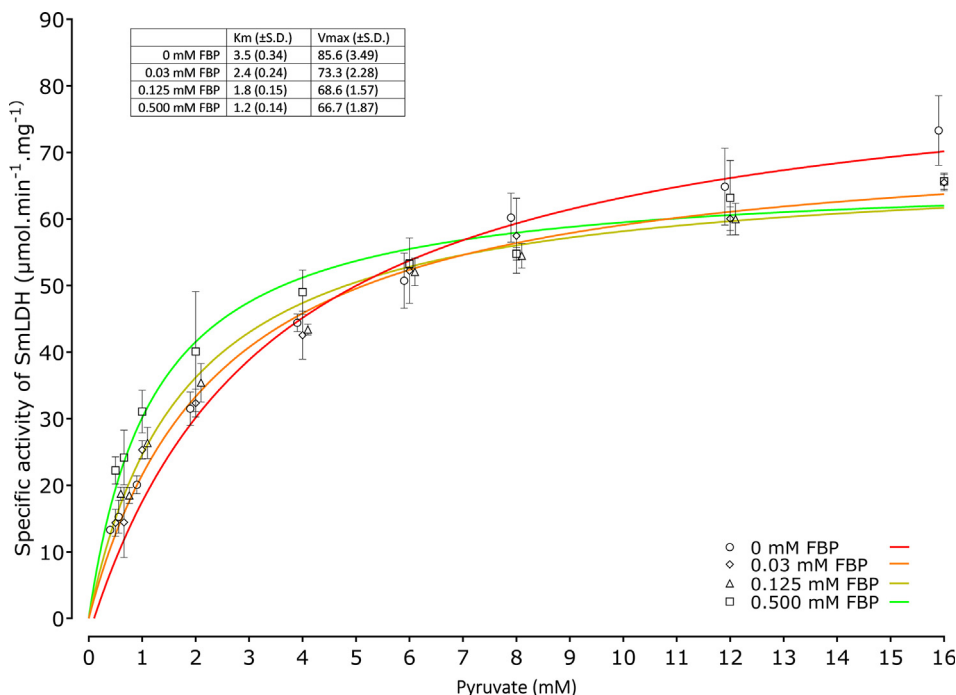


Fig. 4. The effect of fructose-1,6-bisphosphate (FBP) on the Km(pyruvate) of recombinant *Schistosoma mansoni* lactate dehydrogenase (r-SmLDH). Enzymatic activity of r-SmLDH was determined at different pyruvate concentrations (0.5–16 mM) and FBP concentrations (0–0.5 mM). The Km (mM) towards pyruvate, and Vmax (µmol.min⁻¹.mg⁻¹) were determined via a direct linear plot. All measurements were performed in triplicate; shown are the averages ± S.D.

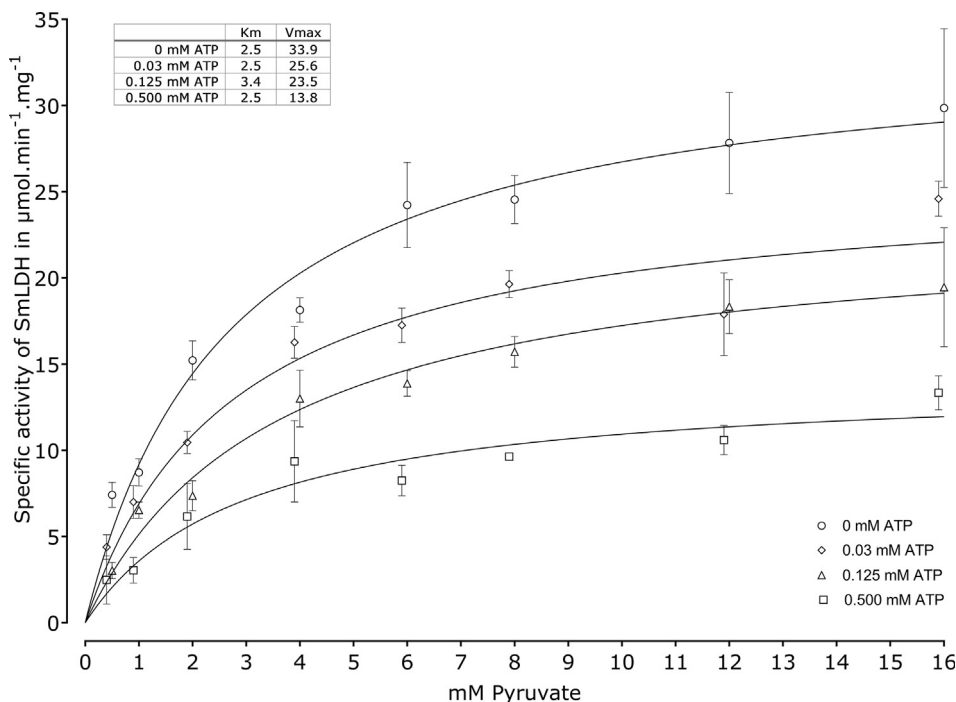


Fig. 5. The effect of ATP on the Vmax and Km(pyruvate) of recombinant *Schistosoma mansoni* lactate dehydrogenase (r-SmLDH). Enzymatic activity of r-SmLDH was determined at different pyruvate concentrations (0.5–16 mM) and ATP concentrations (0–0.5 mM). The Km (mM) and Vmax (µmol.min⁻¹.mg⁻¹) were determined via direct linear plot. All measurements were performed in triplicate; shown is the average ± S.D.

that result in SmLDH and bacterial LDHs being regulated by FBP compared with the FBP-insensitive eukaryotic LDHs (Fig. 6).

Val187 faces into a very hydrophobic environment (Leu175, Leu180, Val182) which is quite well conserved between prokary-

otes and eukaryotes (Fig. 1A). X-ray structures of eukaryote LDHs show Cys187 filling that same pocket without any significant conformational change. The Tyr190Trp mutation would be expected to hamper FBP binding as (based on the modeled side-chain posi-

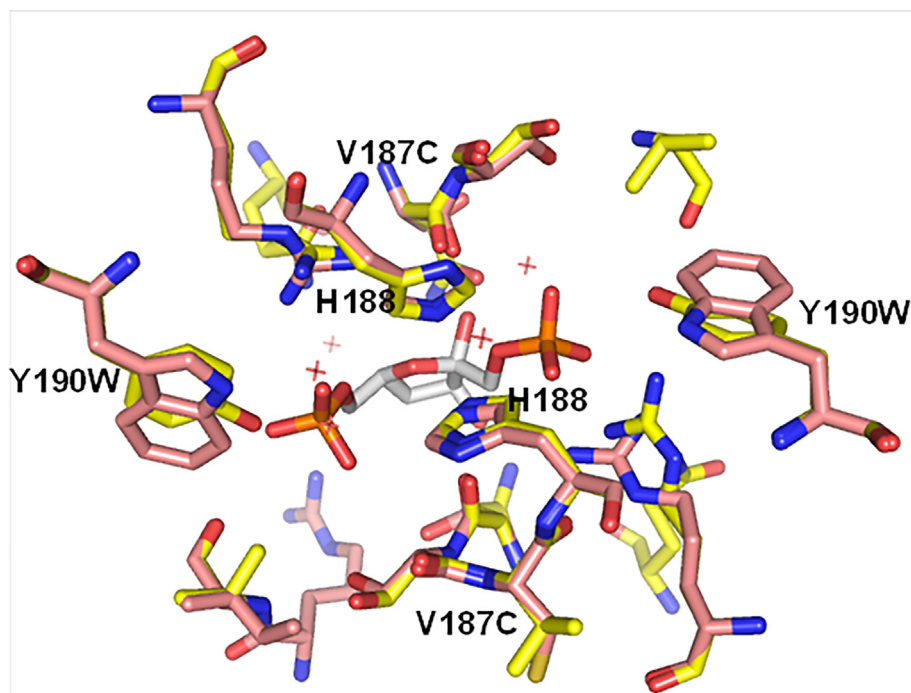


Fig. 6. Allosteric site of schistosomal lactate dehydrogenase (SmLDH) modeled on human LDH. Overlay of model SmLDH (yellow (light grey)) threaded on X-ray structure of human LDH (1t2f, salmon (medium grey)). fructose-1,6-bisphosphate (FBP) is from the *Bacillus* structure and is coloured with carbon in white, phosphorous in orange (dark grey) and oxygen in red (very dark grey). Protein residues were selected that were within 5 Å from the modeled FBP viewed down the approximate two-fold rotation axis relating two chains of the tetramer.

tions) there would be a loss of the favorable Tyr hydrogen bonds with the phosphate groups at either end of FBP (with a modeled distance of ≈ 2.6 Å). In contrast, a best model of the large hydrophobic side chain of Trp190 makes unfavorably short van der Waals contacts of less than 3.8 Å with the phosphates.

An overlay of the BsLDH structure (pdb code 3PQD) onto the model of SmLDH showed that the FBP molecule identified in 3PQD could be accommodated in the anion pocket without any steric clashes. To investigate the potential binding modes of FBP in the anion pocket of SmLDH, the docking program Vina (Trott and Olson, 2010) was used to identify a number of energetically favorable poses similar to that identified in the BsLDH crystal structure. Vina was also used to explore the possibility that ATP could bind in the same anion pocket and compete with FBP. A number of energetically favorable poses were identified, showing that indeed the SmLDH model could easily accommodate ATP (Supplementary Fig. S4).

SmLDH has an N-terminal extension of 15 residues in common with the eukaryotic LDHs. This tail sequence does show some amino acid differences compared with the majority of eukaryotic sequences (Supplementary Fig. S2). A model of this N-terminal tail based on the hLDH structure (1T2F) was generated suggesting that the tail could behave in the same way as in hLDH by wrapping around and stabilizing the tetramer (Supplementary Fig. S5).

Once AlphaFold2-Multimer became available (Mirdita et al., 2022; Richard et al., 2022), the amino acid sequence of SmLDH was used as a starting point to generate a third tetrameric 3D model and compared with the template-based tetramers generated using MODELLER. Gratifyingly, the models were very similar with an RMSfit of 1.1 Å for the 1328 C α atoms of the tetramer (Winn et al., 2011). Fitting the individual chains (using 326 C α atoms) gave smaller RMSD values of 0.6 Å. The close similarity of the models generated by these two independent approaches suggests that the structural models are robust and reliable. Both the Modeller and AlphaFold models position the key side chain resi-

dues in very similar conformations in the FBP pocket (Supplementary Fig. S6).

3.5. Kinetic modeling of the carbohydrate metabolism in *S. mansoni*

To investigate what could be the physiological role of the allosteric regulation of schistosome LDH in the different environmental conditions that the parasite encounters, we created a kinetic model of eukaryotic glycolysis in which we varied the allosteric regulation of LDH. Fig. 2 shows the scheme of the carbohydrate metabolism of *S. mansoni* that we modeled. For SmLDH we fitted parameters to a rate equation (see for choice of equation Supplementary Data S1, section 2) using data from six in vitro experiments with r-SmLDH under diverse substrate concentrations. The resulting parameterized equation was able to realistically capture all experimental data simultaneously (Supplementary Fig. S1).

Due to the limited available kinetic data for the other *S. mansoni* enzymes, we used as a scaffold the well-established glycolysis model for the eukaryote *Saccharomyces cerevisiae* (van Eunen et al., 2012) and adjusted it with *S. mansoni* (kinetic) information where possible (for more information see Supplementary Data S1, section 1). To make our simulations less dependent on accurate parameter values, we explicitly took parameter uncertainty (Achcar et al., 2012, 2013) into account in our analysis. In every analysis, we made 1000 versions of the model with slightly different values for each of the parameters and different starting levels for intermediary metabolites.

To probe the role of the inhibition by ATP and activation by FBP, we made four model versions with four variations in the kinetic properties of LDH (Fig. 7). The ‘Schisto’ model has inhibition of LDH by ATP as well as activation by FBP; in the ‘FBP’ model LDH is only regulated (activated) by FBP; in the ‘ATP’ model LDH is only regulated (inhibited) by ATP; and in the fourth model (‘None’) LDH is not allosterically regulated.

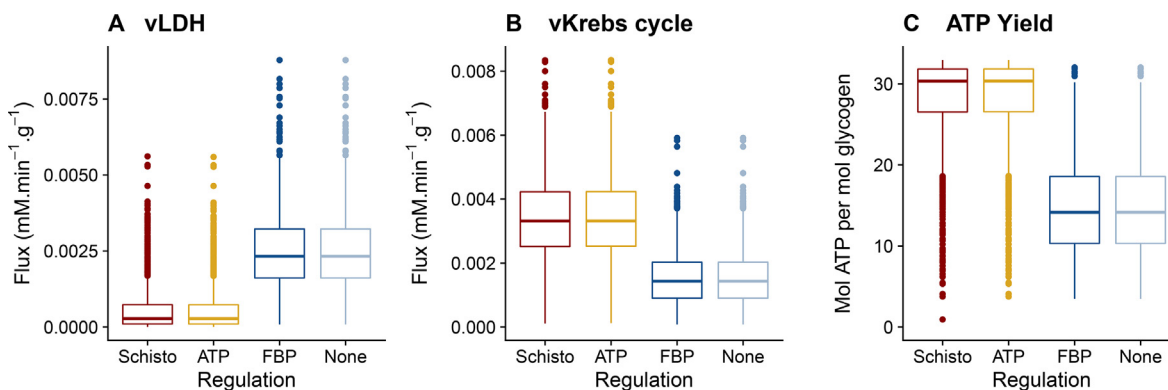


Fig. 7. ATP yield and steady-state enzyme rates (v) of lactate dehydrogenase (LDH) and the Krebs cycle at 0 mM extracellular glucose in *Schistosoma mansoni* models with LDHs with different allosteric properties. Schisto \equiv SmLDH inhibited by ATP and activated by FBP, ATP \equiv LDH with only ATP inhibition, FBP \equiv LDH with only activation by FBP, none \equiv LDH with no allosteric effectors. Data for these boxplots were obtained by simulating 1000 models: for each individual model the parameter values were sampled from probability distributions (see [Supplementary Data S1, section 2](#)). If a steady-state solution was flagged as invalid, a time course of 7 days was done and the last value was recorded. This value was chosen because no more variations could be observed by plotting concentrations over time for a model parameterized by the mean value of the posterior distribution of unmeasured parameters.

We first analyzed the four models under the cercarial freshwater conditions: no external glucose is available and glycogen is the sole carbon source. [Supplementary Fig. S7](#) shows the steady-state values for all enzyme rates and metabolite concentrations in the four models of LDH. The four models mostly had similar steady-state levels for metabolites and rates, but there was a clear difference in the rates of LDH ([Fig. 7A](#)) and the Krebs cycle ([Fig. 7B](#)). The FBP model had a higher rate of LDH (vLDH) and a lower rate of the Krebs cycle (vKrebs), and hence a lower yield of ATP from glycogen-derived glucose ([Fig. 7C](#)). Clearly, the Schisto model and

the ATP model, which both have ATP inhibition of LDH, degraded the glycogen more to carbon dioxide via the Krebs cycle than occurred in the FBP model. The FBP model behaved the same as a model with a non-allosterically regulated LDH (the ‘none’ model). This is in line with the finding that the FBP concentration is low in all models under freshwater conditions, while the ATP concentration is within the range that inhibits LDH for the Schisto model and the ATP model ([Supplementary Fig S7](#)). Together, the results from these simulations suggest that ATP inhibition of LDH is essential to prevent fermentation of the endogenous glycogen reserve to

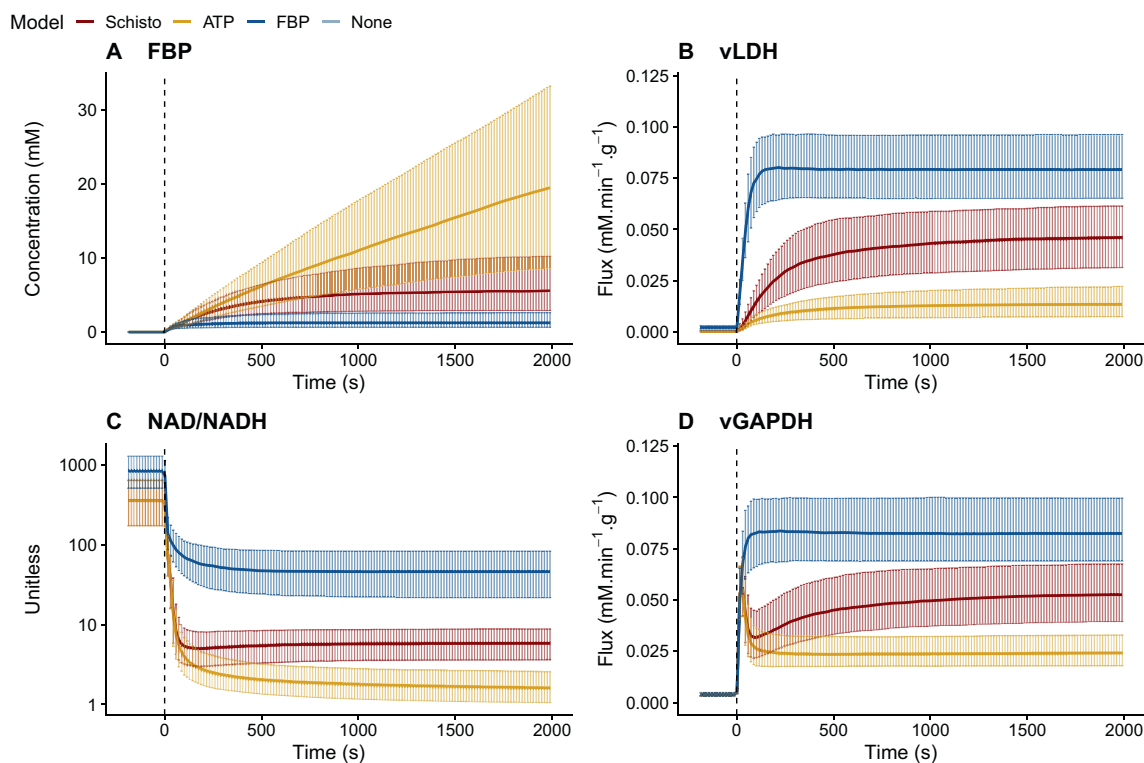


Fig. 8. Effect of a sudden shift from 0 mM to 5.5 mM extracellular glucose in *Schistosoma mansoni* models with lactate dehydrogenases (LDHs) with different allosteric properties. The three models: Schisto (red (dark grey)) \equiv SmLDH inhibited by ATP and activated by fructose-1,6-bisphosphate (FBP), ATP (yellow (light grey)) \equiv LDH with only ATP inhibition, FBP (blue (medium grey)) \equiv LDH with only activation by FBP. Data for these graphs were obtained by simulating 1000 models: for each model, the parameter values were sampled from probability distributions (see [Supplementary Data S1, section 2](#)). Shown is each median (solid line) with their 25% and 75% quantiles (shading). From a steady-state at 0 mM of extracellular glucose, at $t = 0$ s the extracellular glucose concentration was set to 5.5 mM and a time-course was simulated for 2000 s.

lactate. There does not seem to be a metabolic function for FBP activation of LDH when the parasite lives in freshwater conditions and is solely dependent on glycogen as a carbon source.

For the next simulations, we focused on the three models with one or two allosteric regulators (ATP and/or FBP). We switched the models from a steady state in freshwater (no glucose) to 5.5 mM glucose, mimicking entry into the host, and computed a time course for all enzyme rates and metabolite levels (Supplementary Fig. S8). The absence of FBP activation of LDH in the ATP model led to continuously accumulating levels of intracellular FBP upon the increase in glucose at $t = 0$ (Fig. 8A). The rate of LDH (vLDH; Fig. 8B) shows that upon this sudden increase in glucose availability, the ATP model was unable to increase vLDH as much as the other two models. The FBP model reached an even higher rate of LDH than the Schisto model, but it appeared that the rate that LDH was able to reach in the Schisto model was sufficient to control the increase of FBP.

The accumulation of FBP in the ATP model was the result of an imbalance in the rates of upper and lower glycolysis (see for a more elaborate explanation in Supplementary Data S1, section 1). A possible explanation for this imbalance comes from the crosstalk between LDH and GAPDH via the NAD^+/NADH ratio. In the reaction catalyzed by LDH, electrons of NADH are used to reduce pyruvate to lactate. The lower rate of LDH in the ATP model results in a low NAD^+/NADH ratio (Fig. 8C) and a lower rate of GAPDH (Fig. 8D). This, in turn, leads to an accumulation of FBP upstream of GAPDH. Overall, these results indicate that the FBP activation of LDH is important to cope with a sudden increase in glucose availability, but only in the context of an LDH that is inhibited by ATP. Inhibition of LDH by ATP, on the other hand, is an advantage in *S. mansoni* as it prevents fermentation of the limited glycogen reserves to lactate in the free-living stages.

4. Discussion

Here we present a detailed study of a eukaryotic LDH that is regulated by ATP and FBP, often seen in prokaryotes, but not well-known in eukaryotes. By combining data collected from affinity-purified LDH of *S. mansoni* and from recombinant expression of this enzyme, we demonstrated that this type of regulation is not restricted to prokaryotes, of which many possess LDH that is regulated by FBP (Garvie, 1980; Iwata and Ohta, 1993; Fushinobu et al., 1996).

In tetrameric L-LDHs, the active site of each subunit is well-conserved across all species. The residues Arg171, His195, Arg109 and Gln102 bind directly to the substrate and position it over the nicotinamide ring of the NADH cofactor which binds in a Rossmann-fold, a conserved protein domain consisting of six-stranded parallel β sheets and four associated α helices. After binding of the coenzyme followed by binding of the substrate, a protein conformational change occurs in which a highly conserved flexible loop (residues 97 to 123) folds down over the active site pocket to bind the substrate and protect catalytically important residues from the solvent (Abad-Zapatero et al., 1987; Goward and Nicholls, 1994). The Asp168 and His195 residues are conserved in all LDHs and this pair forms a proton relay system in the active site and allows the imidazole ring of the histidine to act as both an acid and a base (Goward and Nicholls, 1994) (Fig. 1A and B). The catalytically crucial proton donor residue His195 sits at the tip of a loop (residues 186–202) which also includes the key residues involved in binding FBP, namely Tyr190, His188 and Ser186 (Fig. 1B). It is likely that any distortion of this loop would disturb the positioning of the catalytic His residue and affect enzyme activity.

Our comparison of the kinetic properties of LDH from rabbit muscle with the purified enzyme from adult *S. mansoni* worms, and the recombinant version of it, revealed that whereas rabbit LDH is unaffected by FBP and ATP, both preparations of the schistosomal enzyme were strongly inhibited by ATP, which can be neutralized by FBP.

The *S. mansoni* genome contains one other gene coding for an L-LDH, Smp_038960. This gene codes for a protein 332 amino acids long, which is overall 94.3% identical to the protein encoded by Smp_038950. The two proteins are 100% identical in the region between amino acids 59 and 305, which contains all catalytic domains and regulatory sites. Therefore, isozyme Smp_038960 most likely has the same kinetics as the SmLDH studied in our paper. The LDH we studied, Smp_038950, is expressed throughout the life cycle of *S. mansoni*, while Smp_038960 is only expressed in 24 h schistosomula and not in cercariae nor adult worms (Lu et al., 2018).

In prokaryotic LDHs that are sensitive to FBP, binding of FBP causes a shift from the tense (inactive) to the relaxed (active) state of the enzyme. There are two anion pockets in each LDH tetramer and these lie between two protomers related to each other by a two-fold rotational axis. The conserved residues lining this pocket (marked in Fig. 1B) are Arg173, His188 and Tyr190 from protomer 'A' and the identical residues from the two-fold related protomer 'B'. This results in a deep symmetrical electropositive cavity. Binding of the (approximately two-fold symmetrical) FBP stabilizes the prokaryotic LDH tetramers in an enzymatically active (R-state) conformation (Wigley et al., 1992; Iwata et al., 1994). Prokaryotic LDHs that are insensitive to FBP are characterized by the absence of a histidine at position 188, one of the two FBP-binding sites (see Fig. 1A) (<https://www.uniprot.org/unirule/UR000103159>).

As we (Fig. 3B) and others have shown (Garvie, 1980; Brennan et al., 1995), FBP has no effect on the catalytic activity of common eukaryotic LDH despite the presence of a deep and well-defined anion binding pocket. Intriguingly, the anion pocket is also quite well conserved in eukaryotic LDH but is not occupied by FBP. However, of the more than 40 eukaryotic LDH X-ray structures available in the protein database (<https://www.rcsb.org>) (Berman et al., 2000) the anion pocket is frequently occupied by a variety of anions including small sulfate or phosphate ions or larger organic anions including citrate. The three carboxyl groups of citrate have been shown in a number of enzyme structures to provide a potential mimic for the three phosphates of ATP (Wenger et al., 2013; Georgescauld et al., 2014; Chandran et al., 2015). This suggests that the inhibition of SmLDH and many bacterial LDHs by ATP could be the result of direct competition of FBP and ATP binding to the anion pocket; a suggestion further supported by our docking studies (Supplementary Fig. S4). The direct competition of ATP with FBP also fits with the available enzymatic data showing that FBP can out-compete ATP and restore activity (Fig. 3A) while adding large amounts of substrate could not out-compete the ATP (Fig. 5). Therefore, we propose that ATP is binding in the allosteric pocket of SmLDH.

It was shown that the addition of the N-terminal extension from mouse testes LDH to *Thermus thermophilus* LDH causes the prokaryotic enzyme to be partially active without FBP present (Iwata et al., 1994). It was also shown that the removal of the N-terminal extension from rabbit LDH causes an increased sensitivity to sub-optimal pH and temperatures, indicating the importance and stabilizing function of this N-terminal extension (Zheng et al., 2004). SmLDH has an N-terminal extension, but is nevertheless stimulated by FBP and inhibited by ATP. Our model of the anion binding pocket showing the steric effect of the Tyr190Trp mutation probably explains the ability of SmLDH to bind FBP and to be activated by FBP. The schistosomal N-extension is comparable in length to other eukaryotic LDHs, but the sequence is not well

conserved with other eukaryotes (Supplementary Fig. S2). Presumably, the SmlDH extension plays some role in stabilizing the tetramer but may not provide the same level of stabilization seen in other eukaryotes.

Our kinetic modeling studies on glycolysis in *S. mansoni* showed that regulation of the LDH activity is important for the switch in metabolism that occurs when external glucose becomes available when the parasite leaves the aquatic environment and enters the final host. It is not possible to construct a schistosome model in an ideal way as the kinetic properties are not known for all enzymes involved. However, even with the limited experimental data available, modeling provided new insights by explicitly taking parameter uncertainty into account. We show in our analyses that applying uncertainty of the parameters within realistic ranges did not change the conclusions (Achcar et al., 2012).

The - for eukaryotes - rather unique regulatory mechanism of the LDH of *S. mansoni* very well suits the changes in the environments that the parasite encounters during its life cycle. These environments differ greatly in glucose availability. The two free-living stages, cercariae and miracidia, live in water and oxidize their very limited endogenous glycogen stores completely to carbon dioxide via the Krebs cycle, and use oxidative phosphorylation for the maximal production of ATP (Horemans et al., 1991, 1992; Tielens et al., 1992). Our model suggests that prevention of lactate fermentation by the ATP inhibition of LDH ensures the maximal production of ATP, maximizing the chance that the next host is found and entered before glycogen is exhausted. On the other hand, the inhibition of LDH by ATP creates a problem upon the entrance of a host. In such a glycolytic system, the sudden presence of glucose would result in an imbalance in the rates of the upper and the lower part of glycolysis and the accumulation of FBP. However, neutralization of the ATP inhibition of LDH by FBP prevents glycolytic intermediate accumulation when *S. mansoni* schistosomula are confronted with the sudden large increase of glucose in the cytosol of the cells that occurs after entering the final host. Imbalances between the upper and lower parts of glycolysis have been observed experimentally in *S. cerevisiae* regulatory mutants, and were explained by phosphate dependence of GAPDH (van Heerden et al., 2014). Here, the imbalance in the *S. mansoni* model is caused by a low LDH activity translating into low GAPDH activity via the NAD⁺/NADH ratio.

In this parasitic stage of *S. mansoni*, a wasteful fermentative metabolism producing lactate is of no concern to the parasite, as substrates are now provided by the host. The *S. mansoni* LDH is well suited to facilitating the delicate orchestration of these switches in energy metabolism, as the metabolic switch is instantaneous and occurs immediately after penetration of the mammalian host. This implies that schistosomes have to be prepared for that switch and regulation of glycolysis by adjusting gene expression is not an option.

LDH is not the only enzyme in the core metabolism of *S. mansoni* that has unusual properties. In contrast to the enzyme of other eukaryotes, *S. mansoni* hexokinase is relatively insensitive to its product, glucose-6-phosphate (Tielens et al., 1994; Armstrong et al., 1996). Simulations with our model indicate that lowering the K_i of HK for G6P (i.e. stronger product inhibition) in the ATP model would lead to lower steady-state levels of FBP (Supplementary Fig. S9). A K_i value of 0.02 mM as reported for mammalian HK (Wilson, 2003) would limit the rise of [FBP] in the ATP-model to a steady state level of ≈ 2 mM. Product inhibition of the first kinases of glycolysis would be an alternative to prevent a too-high influx of glucose and thus the imbalance in the rates of upper and lower glycolysis which results in the accumulation of intermediates of upper glycolysis.

The homolactic type of energy metabolism of *S. mansoni* (and of closely related trematodes such as *Schistosoma japonicum*, *Clonorchis sinensis* and *Opisthorchis viverrini*) that relies predominantly

on LDH, is an interesting drug target, especially as small molecular inhibitors directed against LDH are being investigated as possible drugs against cancer cell metabolism (Le et al., 2010; Porporato et al., 2011).

It was suggested already in 1954 that the active site of LDH of *S. mansoni* differs from that of mammalian LDH (Mansour et al., 1954). Some details of the difference and its implications for the bio-energetic transitions during the life cycle of *S. mansoni* are now known.

CRedit authorship contribution statement

Michiel L. Bexkens: Formal analysis, Investigation, Writing – original draft. **Olivier M.F. Martin:** Methodology. **Jos M. van den Heuvel:** Formal analysis, Investigation. **Marion G.J. Schmitz:** Formal analysis, Investigation. **Bas Teusink:** Supervision. **Barbara M. Bakker:** Supervision. **Jaap J. van Hellemond:** Conceptualization, Formal analysis, Investigation. **Jurgen R. Haanstra:** Conceptualization, Supervision, Writing – original draft, Writing – review & editing. **Malcolm D. Walkinshaw:** Methodology, Writing – original draft. **Aloysius G.M. Tielens:** Conceptualization, Supervision, Writing – original draft, Writing – review & editing.

Acknowledgements

We thank Josan Yauw (VU Amsterdam) for her work on the initial versions of the model and Brett Olivier for valuable comments on the model description. The investigations were supported by the Netherlands Foundation for Chemical Research (SON) with financial aid from the Netherlands Organization for Scientific Research (NWO).

Appendix A. Supplementary data

Supplementary data to this article can be found online at <https://doi.org/10.1016/j.ijpara.2024.03.005>.

References

- Abad-Zapatero, C., Griffith, J.P., Sussman, J.L., Rossmann, M.G., 1987. Refined crystal structure of dogfish M4 apo-lactate dehydrogenase. *J. Mol. Biol.* 198, 445–467.
- Achcar, F., Kerkhoven, E.J., SilicoTryp, C., Bakker, B.M., Barrett, M.P., Breitling, R., 2012. Dynamic modelling under uncertainty: the case of *Trypanosoma brucei* energy metabolism. *PLoS Comput. Biol.* 8, e1002352.
- Achcar, F., Barrett, M.P., Breitling, R., 2013. Explicit consideration of topological and parameter uncertainty gives new insights into a well-established model of glycolysis. *FEBS J.* 280, 4640–4651.
- Adams, M.J., Liljas, A., Rossmann, M.G., 1973. Functional anion binding sites in dogfish M4 lactate dehydrogenase. *J. Mol. Biol.* 76, 519–528.
- Armstrong, R.L., Wilson, J.E., Shoemaker, C.B., 1996. Purification and Characterization of the Hexokinase from *Schistosoma mansoni*, Expressed in *Escherichia coli*. *Prot. Exp. Purif.* 8, 374–380.
- Bensadoun, A., Weinstein, D., 1976. Assay of proteins in the presence of interfering materials. *Anal. Biochem.* 70, 241–250.
- Berman, H.M., Westbrook, J., Feng, Z., Gilliland, G., Bhat, T.N., Weissig, H., Shindyalov, I.N., Bourne, P.E., 2000. The protein data bank. *Nucleic Acids Res.* 28, 235–242.
- Birkof, J., Fernley, R., Bradshaw, R., Banaszak, L., 1982. Amino acid sequence homology among the 2-hydroxyacid dehydrogenase: mitochondrial and cytoplasmic malate dehydrogenase form a homologous system with lactate dehydrogenase. *PNAS* 79, 6166–6170.
- Brennan, S., Holder, J., Baldwin, J., 1995. An unusual fructose 1,6-bisphosphate-activated lactate dehydrogenase from the ascidian *Pyura stolonifera*. *Comp. Biochem. Physiol. B Biochem. Mol. Biol.* 110, 689–695.
- Bruce, J.L., Weiss, E., Stirewalt, M.A., Lincicome, D.R., 1969. *Schistosoma mansoni*: glycogen content and utilization of glucose, pyruvate, glutamate, and citric acid cycle intermediates by cercariae and schistosomules. *Exp. Parasitol.* 26, 29–40.
- Bueding, E., 1950. Carbohydrate metabolism of *Schistosoma mansoni*. *J. Gen. Physiol.* 33, 475–495.
- Chandran, A.V., Prabu, J.R., Nautiyal, A., Patil, K.N., Muniyappa, K., Vijayan, M., 2015. Structural studies on *Mycobacterium tuberculosis* RecA: molecular plasticity and interspecies variability. *J. Biosci.* 40, 13–30.

- Esvar, N., Eramian, D., Webb, B., Shen, M.Y., Sali, A., 2008. Protein structure modeling with MODELLER. *Methods Mol. Biol.* 426, 145–159.
- Eventoff, W., Rossmann, M.G., Taylor, S.S., Torff, H.J., Meyer, H., Keil, W., Kiltz, H.H., 1977. Structural adaptations of lactate dehydrogenase isozymes. *PNAS* 74, 2677–2681.
- Fushinobu, S., Kamata, K., Iwata, S., Sakai, H., Ohta, T., Matsuzawa, H., 1996. Allosteric activation of L-lactate dehydrogenase analyzed by hybrid enzymes with effector-sensitive and -insensitive subunits. *J. Biol. Chem.* 271, 25611–25616.
- Garvie, E.L., 1980. Bacterial lactate dehydrogenases. *Microbiol. Rev.* 44, 106–139.
- Georgescauld, F., Moynie, L., Habersetzer, J., Dautant, A., 2014. Structure of *Mycobacterium tuberculosis* nucleoside diphosphate kinase R80N mutant in complex with citrate. *Acta Crystallogr. F Struct. Biol. Commun.* 70, 40–43.
- Goward, C.R., Nicholls, D.J., 1994. Malate dehydrogenase: a model for structure, evolution, and catalysis. *Prot. Sci.* 3, 1883–1888.
- Grau, U.M., Trommer, W.E., Rossmann, M.G., 1981. Structure of the active ternary complex of pig heart lactate dehydrogenase with S-lac-NAD at 2.7 Å resolution. *J. Mol. Biol.* 151, 289–307.
- Horemans, A.M., Tielens, A.G., van den Bergh, S.G., 1991. The transition from an aerobic to an anaerobic energy metabolism in transforming *Schistosoma mansoni* cercariae occurs exclusively in the head. *Parasitology* 102 (Pt 2), 259–265.
- Horemans, A.M., Tielens, A.G., van den Bergh, S.G., 1992. The reversible effect of glucose on the energy metabolism of *Schistosoma mansoni* cercariae and schistosomula. *Mol. Biochem. Parasitol.* 51, 73–79.
- Iwata, S., Kamata, K., Yoshida, S., Minowa, T., Ohta, T., 1994. T and R states in the crystals of bacterial L-lactate dehydrogenase reveal the mechanism for allosteric control. *Nat. Struct. Biol.* 1, 176–185.
- Iwata, S., Ohta, T., 1993. Molecular basis of allosteric activation of bacterial L-lactate dehydrogenase. *J. Mol. Biol.* 230, 21–27.
- Le, A., Cooper, C.R., Gouw, A.M., Dinavahi, R., Maitra, A., Deck, L.M., Royer, R.E., Vander Jagt, D.L., Semenza, G.L., Dang, C.V., 2010. Inhibition of lactate dehydrogenase A induces oxidative stress and inhibits tumor progression. *PNAS* 107, 2037–2042.
- Lloyd, G.M., 1983. A fructose bisphosphate activated lactate dehydrogenase in the liver fluke *Fasciola hepatica*. *Mol. Biochem. Parasitol.* 7, 237–246.
- Lu, Z., Zhang, Y., Berriman, M., 2018. A web portal for gene expression across all life stages of *Schistosoma mansoni*. *bioRxiv* 308213.
- Madern, D., 2002. Molecular evolution within the L-malate and L-lactate dehydrogenase super-family. *J. Mol. Evol.* 54, 825–840.
- Mansour, T.E., Bueding, E., Stavitsky, A.B., 1954. The effect of a specific antiserum on the activities of lactic dehydrogenase of mammalian muscle and of *Schistosoma mansoni*. *Br. J. Pharmacol. Chemother.* 9, 182–186.
- McKinney, W., 2011. pandas: a foundational Python library for data analysis and statistics. *Python for high performance and scientific computing* 14, 1–9. https://www.researchgate.net/publication/265194455_pandas_a_Foundational_Python_Library_for_Data_Analysis_and_Statistics
- Mirdita, M., Schütze, K., Moriawaki, Y., Heo, L., Ovchinnikov, S., Steinegger, M., 2022. ColabFold: making protein folding accessible to all. *Nat. Methods* 19, 679–682.
- Olivier, B.G., Rohwer, J.M., Hofmeyr, J.H., 2005. Modelling cellular systems with PySCeS. *Bioinformatics* 21, 560–561.
- Pérez, F., Granger, B.E., 2007. IPython: a system for interactive scientific computing. *Comput. Sci. Eng.* 9, 21–29.
- Porporato, P.E., Dhup, S., Dadhich, R.K., Copetti, T., Sonveaux, P., 2011. Anticancer targets in the glycolytic metabolism of tumors: a comprehensive review. *Front. Pharmacol.* 2, 49.
- Read, J.A., Winter, V.J., Eszes, C.M., Sessions, R.B., Brady, R.L., 2001. Structural basis for altered activity of M- and H-isozyme forms of human lactate dehydrogenase. *Proteins* 43, 175–185.
- Richard, E., Michael, O.N., Alexander, P., Natasha, A., Andrew, S., Tim, G., Augustin, Ž., Russ, B., Sam, B., Jason, Y., Olaf, R., Sebastian, B., Michal, Z., Alex, B., Anna, P., Andrew, C., Kathryn, T., Rishub, J., Ellen, C., Pushmeet, K., John, J., Demis, H., 2022. Protein complex prediction with AlphaFold-Multimer. *bioRxiv*. 2021.2010.2004.463034.
- Tielens, A.G., 1997. Biochemistry of trematodes. In: Fried, B., Graczyk, T.K. (Eds.), *Advances in Trematode Biology*. CRC Press, Boca Raton, Florida, pp. 309–343.
- Tielens, A.G., van Oordt, B.E., van den Bergh, S.G., 1989. Carbohydrate metabolism in adult schistosomes of different strains and species. *Int. J. Parasitol.* 19, 447–449.
- Tielens, A.G., van de Pas, F.A., van den Heuvel, J.M., van den Bergh, S.G., 1991. The aerobic energy metabolism of *Schistosoma mansoni* miracidia. *Mol. Biochem. Parasitol.* 46, 181–184.
- Tielens, A.G., Horemans, A.M., Dunnewijk, R., van der Meer, P., van den Bergh, S.G., 1992. The facultative anaerobic energy metabolism of *Schistosoma mansoni* sporocysts. *Mol. Biochem. Parasitol.* 56, 49–57.
- Tielens, A.G., van den Heuvel, J.M., van Mazijk, H.J., Wilson, J.E., Shoemaker, C.B., 1994. The 50-kDa glucose 6-phosphate-sensitive hexokinase of *Schistosoma mansoni*. *J. Biol. Chem.* 269, 24736–24741.
- Trott, O., Olson, A.J., 2010. AutoDock Vina: improving the speed and accuracy of docking with a new scoring function, efficient optimization, and multithreading. *J. Comput. Chem.* 31, 455–461.
- Van Der Walt, S., Colbert, S.C., Varoquaux, G., 2011. The NumPy array: a structure for efficient numerical computation. *Comput. Sci. Eng.* 13, 22–30.
- van Eunen, K., Kiewiet, J.A.L., Westerhoff, H.V., Bakker, B.M., 2012. Testing biochemistry revisited: how in vivo metabolism can be understood from in vitro enzyme kinetics. *PLoS Comput. Biol.* 8, e1002483.
- van Grinsven, K.W., van Hellemond, J.J., Tielens, A.G., 2009. Acetate:succinate CoA-transferase in the anaerobic mitochondria of *Fasciola hepatica*. *Mol. Biochem. Parasitol.* 164, 74–79.
- van Heerden, J.H., Wortel, M.T., Bruggeman, F.J., Heijnen, J.J., Bollen, Y.J., Planque, R., Hulshof, J., O'Toole, T.G., Wahl, S.A., Teusink, B., 2014. Lost in transition: start-up of glycolysis yields subpopulations of nongrowing cells. *Science* 343, 1245–1249.
- Van Oordt, B.E.P., Tielens, A.G., Van den Bergh, S.G., 1989. Aerobic to anaerobic transition in the carbohydrate-metabolism of *Schistosoma mansoni* cercariae during transformation in vitro. *Parasitology* 98, 409–415.
- Wenger, J., Klinglmayr, E., Frohlich, C., Eibl, C., Gimeno, A., Hessenberger, M., Puehringer, S., Daumke, O., Goettig, P., 2013. Functional mapping of human dynamin-1-like GTPase domain based on x-ray structure analyses. *PLoS One* 8, e71835.
- Wickham, H., 2016. Getting started with ggplot2. *ggplot2: Elegant Graphics for Data Analysis*. Springer, Cham.
- Wigley, D.B., Gamblin, S.J., Turkenburg, J.P., Dodson, E.J., Piontek, K., Muirhead, H., Holbrook, J.J., 1992. Structure of a ternary complex of an allosteric lactate dehydrogenase from *Bacillus stearothermophilus* at 2.5 Å resolution. *J. Mol. Biol.* 223, 317–335.
- Wilson, J.E., 2003. Isozymes of mammalian hexokinase: structure, subcellular localization and metabolic function. *J. Exp. Biol.* 206, 2049–2057.
- Winn, M.D., Ballard, C.C., Cowtan, K.D., Dodson, E.J., Emsley, P., Evans, P.R., Keegan, R.M., Krissinel, E.B., Leslie, A.G., McCoy, A., McNicholas, S.J., Murshudov, G.N., Pannu, N.S., Potterton, E.A., Powell, H.R., Read, R.J., Vagin, A., Wilson, K.S., 2011. Overview of the CCP4 suite and current developments. *Acta Crystallogr. D Biol. Crystallogr.* 67, 235–242.
- Zheng, Y., Guo, S., Guo, Z., Wang, X., 2004. Effects of N-terminal deletion mutation on rabbit muscle lactate dehydrogenase. *Biochemistry (Mosc.)* 69, 401–406.